FFI Norwegian Defence Research Establishment

22/02204

FFI-RAPPORT

Target detection in radars using small neural networks

Jabran Akhtar

Target detection in radars using small neural networks

Jabran Akhtar

Norwegian Defence Research Establishment (FFI) 17 August 2022

Keywords
Radar
Deteksjon
Maskinlæring

FFI report
22/02204

Project number
1588

Electronic ISBN
978-82-464-3437-7

Approvers
Børge Torvik, *Research Manager*
Connie Solberg, *Research Director*

The document is electronically approved and therefore has no handwritten signature.

Summary

Target detection is an essential part of radar systems. An important objective in radar target detection is to satisfy two often contradictory requirements: a high probability of detection with a low false alarm rate. This report proposes and investigates the use of a particular machine learning method to detect targets in range-Doppler images. The application of machine learning in such a context allows the detection procedure to be designed primarily on available data. This can therefore reduce the need to design detection algorithms tailored for different scenarios.

The method proposed in this report follows a two-step approach. In the first step a depreciated detection process is performed which results in a high probability of detection and a very large false alarm rate. In the second step a trained neural network makes a final decision to classify the detection as true or false. The report shows that trained neural networks are capable of identifying false detections with considerable accuracy. These networks can utilize information available in guard cells and Doppler profiles. This allows for a significant reduction in false alarm rate with moderate loss in the probability of detection. With an appropriately designed neural network, an overall improved system performance can be achieved when compared against traditional constant false alarm rate (CFAR) detectors for the specific trained scenarios. The trained scenarios may include land or sea clutter and difficult to detect targets, such as those with low signal to noise ratio, multiple closely spaced targets or targets in clutter edges.

The report is based largely on a previously published paper [1] by the author.

Sammendrag

Måldeteksjon er en viktig oppgave for radarsystemer. En ønsker å tilfredstille to delvis motstridende krav: å oppnå høy deteksjonsevne samtidig med en lav falsk alarmrate. Denne rapporten ser på deteksjon av mål i avstand-dopplerbilder. Vi foreslår en maskinlæringsmetodikk for dette formålet. Bruk av maskinlæring gjør det mulig å utvikle deteksjonsmetoder utelukkende basert på innsamlede data. Dette kan blant annet redusere behov for utvikling av egne deteksjonsalgoritmer for ulike scenarioer.

I denne rapporten foreslås en tostegs prosess for deteksjon. I det første steget gjennomføres deteksjon med en forenklet tradisjonell teknikk. Denne teknikken resulterer i høy deteksjonsevne, men med atskillige falske deteksjoner. I det neste steget tar et trent nevralt nettverk en endelig avgjørelse som klassifiserer deteksjoner som korrekte eller falske. Resultatene av en slik prosess viser at trente nevrale nettverk kan identifisere falske deteksjoner med god nøyaktighet. Nettverket kan anvende tilgjengelig informasjon i naboceller og dopplerprofiler for bedret ytelse. Dette gjør det mulig å redusere i falsk alarmrate med begrenset tap i deteksjonsevne. Med et tilpasset trent nevralt nettverk kan en oppnå økt systemytelse sammenlignet med tradisjonelle CFAR (konstant falsk alarm rate) deteksjonsmetoder. Scenarioene for opptrening kan inneholde ulik typer clutter og mål, som det kan være vanskelig å detektere på grunn av lav signal-til-støyforhold, multiple nærliggende objekter eller mål i clutterkanter.

Denne rapporten er hovedsakelig basert på en publisert artikkel [1] av forfatteren.

Contents

1 Introduction

Discriminating targets from background noise and interference is a fundamental task of most radar systems. Targets need to be differentiated with high probability of detection (P_D) and simultaneously the detection methodology should offer a low false alarm rate (P_{FA}). The radar detection problem is complicated by possible factors such as multiple closely spaced targets, the presence of clutter and clutter edges in vicinity of targets. Target detection has been studied heavily over the years and a large number of techniques have been suggested. One particular class of algorithms, which also sufficiently satisfy the constant false alarm rate (CFAR) property, include CA (Cell Averaging), GO (Greatest Of) and SO (Smallest Of) CFAR sliding window methods with several proposed variants [2, 3, 4, 5, 6, 7, 8, 9]. Importantly, these detectors aim to provide an adaptive mean to calculate the detection threshold as fixed thresholds are inadequate in case of complex and dynamic surroundings. In the literature, a wide variety of alternative detection methods have also been proposed for specific environmental conditions where the detectors are tailored with respect to assorted target and clutter distributions and applicable secondary data is made use of [10, 11, 12, 13, 14, 15]. These methods often rely on estimation of distribution parameters, the covariance matrices and are dependent upon accurate estimation of these figures.

The use of machine learning has gained much attention over the years and these techniques have also been discussed in radar contexts for target detection [16, 17, 18, 19, 20, 21, 22, 23, 24, 25, 26, 27, 28]. Particularly, [23] investigated the use of deep convolutional networks to improve target detection while [25] employed autoencoders for the same task. In [21, 22, 29], the authors proposed training of feedforwarding neural networks (NN) to emulate various CFAR detectors while concurrently aiming to reduce the number of false detections. The trained neural networks were demonstrated to be effective in reproducing the detection algorithms and in reducing the false alarm rate with some loss in probability of detection. Nevertheless, the proposed approaches also left open several questions, such as what features do the networks require to distinguish between true and false detections, are there circumstances where they do not operate well, how many layers should a network have and what would be the maximum potential for such a trained neural network? Several disadvantages with the previous techniques have also been poined out. For instance, the neural networks were required to learn and implement the CFAR detection process as well as discriminating between true and false detections resulting in an interweave training procedure with lesser degree of specialization. Training a network to behave like a standard CFAR method, but with additional constrains results in trade-off between the two requirements of obtaining a high probability of detection and a low false alarm rate. The training method can thus mainly only be used to define detectors with different compromises than the original starting point detector. The previous strategy was also found to be incapable of further generalization with regard to sophisticated type of detectors who e.g. require sorting of entries. Finally, processing every sliding window sample through a full neural network is a computational expensive procedure, compared to a standard CFAR test, and other strategies who can be developed would therefore be of great practical interest.

Practically, development of more sophsicated detection methods, based on neural networks or other techniques, is a necessary requirement to

- detect and track weak targets with low SNR
- detect and track multiple closely spaced targets (such as drones)
- detect and track targets in clutter environments.

– increase the operational range of radars.

Concrete examples can be linked with for example unmanned aerial drones, these aircaft are typically small with correspondingly small radar cross section, they can fly in formations close to each others at low velocities and at low altitudes. Accurate detection of these targets in varying conditions therefore remains a challengig task.

The method presented in this technical report presents a generic methodology on how to train and perform the CFAR detection process in combination with feedforwarding neural networks. The initial detection process is proposed carried out conventionally by making use of an amended, rudimentary, sliding window detector, and only positive detections are to be processed by the neural network. The neural network thus acts as a specialized binary classifier between true and false detections. In a simplified manner, the main parts of this process are visualized in figure 1.1.

The leading detection strategy in the overall setup is based on a modified version of censored mean SO-CFAR with the objective to force the detector to provide a high probability of detection. In the suggested SO-CFAR construction, a number of the largest elements in the sliding window are censored which makes it viable to detect in tangled conditions such as multiple closely spaced targets as well as enclosed targets in clutter edges. The downside of this is an exceedingly high false alarm rate which is where the neural network steps in and aims to curtail it to acceptable levels. In order to achieve a high probability of correct target detection, it is shown that simply using the CFAR sliding window samples is not sufficient rather the target spread in Doppler contains important discriminatory information and contributes positively if integrated by the neural network. By linking together different strategies in an appropriate training session it is shown that a high level of P_D can be achieved with a satisfactory low P_{FA} for the type of scenarios the network has been trained on. On the other hand, if only elementary CFAR window data, also excluding guard cells, is allotted to train a neural network then in a noise-only situation the networks can converge towards a traditional CFAR detection strategy. The presented techniques would permit a radar sensor to adapt the detection process to its surroundings based on learned collected or simulated data.

To demonstrate the potential advantages and disadvantages, this reports displays simulations performed over convoluted scenes with multiple closely spaced fluctuating targets and with and without K-distributed clutter. The simulations are performed and evaluated under various parameters and sliding window structures.

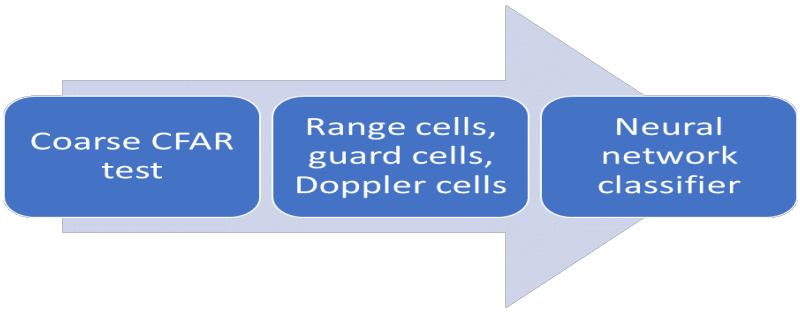

Figure 1.1 The overall detection process.

2 Radar and signal model

This chapter presents a generic structure for a pulsed radar system upon which a sliding window detector can be modeled. The radar is assumed to emit a burst of M waveforms in a coherent processing interval (CPI). The targets are assumed to be slowly fluctuating with a distribution, such as Swerling 1, where the values vary randomly across different dwells but with a given mean signal-to-noise ratio (SNR) and signal-to-clutter ratio (SCR). For each CPI, the radar processing unit performs a tapered Fourier transform over each range bin to construct a range-Doppler map represented by an $M \times R$ complex matrix $\mathbf{D}(t, \omega)$. $t = 1, 2, ..., R$ is the discrete fast-time parameter with respect to different time delays (range cells) while $\omega = 1, ..., M$ represents the Doppler cells.

To perform a detection, each individual cell of the range-Doppler map is evaluated one by one. The detector takes the square law range samples of the map $\mathbf{D}$, $\hat{\mathbf{D}}(t, \omega) = |\mathbf{D}(t, \omega)|^2 \ \forall \ t, \omega$, and a sliding window of size $2N + 2G + 1$ is moved across, $\hat{t} = 1 + N + G, ..., R - N - G$ and $\hat{\omega} = 1, ..., N$ excluding the edges. G refers to the number of guard cells and N to the number of averaging cells on each side of the CFAR window (an illustration is later given in figure 3.1). The $2N + 2G + 1$ samples in range specified by the window are extracted in

$$x(u) = \hat{\mathbf{D}}(\hat{t} - N - G : \hat{t} + N + G, \hat{\omega}), \ u = 1, 2, ..., 2N + 2G + 1, \tag{2.1}$$

and the cell in the middle of the window, $x(N + G + 1)$, cell under test (CUT), is compared against a scaled average, γ, to determine if conditions for declaring a detection are satisfied. G number of gap cells immediately to the right and left of CUT are discarded when computing the average to avoid target leakage and neutralize the impact of sidelobes. A detection is declared if

$$x(u)_{|u=CUT} > \gamma \ K, \tag{2.2}$$

where K is a specified threshold.

The background average, γ, plays a central role in the detection process and may be computed through a variety of methods. In (Cell Averaging) CA-CFAR the average is composed of all available $2N$ cells,

$$\gamma = \frac{1}{2N}\left(\sum_{k=1}^{N} x(k) + \sum_{k=N+2G+2}^{2N+2G+1} x(k)\right), \tag{2.3}$$

which corresponds to a maximum likelihood estimate under homogeneous assumptions [30, 6] but can also be attempted applied under other conditions. Other alternatives, GO (Greatest Of) GO-CFAR and (Smallest Of) SO-CFAR can be implemented where two averages are computed based on N reference values each from the left and right side of the CUT,

$$\gamma_1 = \frac{1}{N}\sum_{k=1}^{N} x(k), \quad \gamma_2 = \frac{1}{N}\sum_{k=N+2G+2}^{2N+2G+1} x(k). \tag{2.4}$$

In GO-CFAR, a conservative approach is taken as the maximum value among the two is selected as the comparable value,

$$\gamma = \max \ (\gamma_1, \gamma_2), \tag{2.5}$$

resulting in typically a slightly lower probability of detection (P_D) alongside reduced false alarm rate. In SO-CFAR, instead, the smallest value is chosen,

$$\gamma = \min \ (\gamma_1, \gamma_2), \tag{2.6}$$

which improves detection in case of clutter edge or in the presence of an additional target on one side of the sliding reference window [31]. This results in a good detectional performance, however, as the interference level is always underestimated a high P_{FA} is to be expected in non-homogeneous conditions. There exists a large number of other methods including censored mean level (CML-CFAR) detectors [32, 33] where the largest samples in the reference windows are excluded before the background mean is computed. Removing the greater values improves detection in presence of multiple close targets but otherwise comes at the expense of P_{FA} due to an undervalued γ estimate. In previous works, [21, 22] it was demonstrated that a neural network could be trained to mimic the classical CFAR detectors with reduced number of incorrect detections but the P_D could not be increased. Building upon this capability one can move forward to a new type of detection process where the detector is altered to provide a very high level of P_D alongside a much enlarged P_{FA}. This can be viewed as the first step in a two part cascaded classification process, where in the first stage, the designated detector synthesizes a very coarse decision. In the second step only positive detections are evaluated by a trained neural network to determine if the bin (CUT) qualifies for a detection or not. The procedure implemented by the secondary network classifier is not contingent upon a particular detector but the first detection upper-bounds the P_D performance of the system and the network is only taught to identify false detections with respect to a given detector. In this text, we limit ourselves to the modified version of the classical SO-CFAR detector as it can be used to demonstrate the applicability on both noise-only and clutter based scenarios. This detector may readily be replaced by other type of detectors; preferably, as long as the detector can be tuned to yield a larger or fewer number of correct and incorrect detections.

3 System design

The methodology of the two-step detection and classification process is described in this chapter.

3.1 Step 1: CMSO-CFAR detector

As the initial first step detector we utilize a modified version of the censored mean level detector combined with SO-CFAR, denoted herein as CMSO-CFAR. In this detector, the N outermost elements of the right and left side of the sliding window $x(u)$ are sorted in two blocks in increasingly order

$$\hat{x}_1(u) = sort(x(1) \ ... \ x(N)) \tag{3.1}$$

and

$$\hat{x}_2(u) = sort(x(N + 2G + 2) \ ... \ x(2N + 2G + 1)). \tag{3.2}$$

From each block only the first P, $1 \leq P \leq N$, lowest value samples are taken into consideration in estimating the two mean averages,

$$\gamma_1 = \frac{1}{P}\sum_{k=1}^{P}\hat{x}_1(k), \quad \gamma_2 = \frac{1}{P}\sum_{k=1}^{P}\hat{x}_2(k). \tag{3.3}$$

The smallest of these two averages is selected $\gamma = \min\ (\gamma_1, \gamma_2)$ as the estimate to be applied by equation (2.2). The performance of this detector will be contingent on the choice of P. A selection of $P = N$ leads to the standard case of SO-CFAR while at the other extreme $P = 1$ implies an unrefined estimate of the background noise or clutter. A small choice of P, nevertheless, is befitting for detection of multiple closely spaced targets and detection in non-homogeneous settings. The reference level γ can be rather forgiving in CMSO-CFAR but operates as a regulator of when it is justifiable to train and evaluate a cell by the neural network. A complementary objective of the detector is to make certain that not the complete range-Doppler map requires inspection by a neural network which would lead to a more computational expensive operation.

3.2 Step 2: neural network classifier

In the second step, all positive outcomes from the initial detector are processed by a neural network. If the detector returns a positive value, only then selected range-Doppler data, from the neighborhood of CUT, is supplied to the network. Consequently, the output from the neural network determines if a target detection at CUT is declared or not.

The aforementioned CMSO-CFAR test is formulated to operate in the range dimension only, however, for the neural network several other choices can be made on what type of data it should be dispensed from the range-Doppler map. We consider three different options, namely O1, O2, and O3 where the data fed into the network is specified by $\mathbf{r}$ and follows:

- O1: $\mathbf{r} = (x(1) \ ... \ x(N),\ x(N + G + 1),\ x(N + 2G + 1) \ ... \ x(2N + 2G + 1))$, $2N + 1$ values corresponding to the sliding window reference cells and the value in CUT
- O2: $\mathbf{r} = (x(1) \ ... \ x(2N + 2G + 1))$, $2N + 2G + 1$ values corresponding to the sliding window reference cells, including guard cells, and the value in CUT

– O3: $\mathbf{r} = (x(1)\ \ldots\ x(2N+2G+1),\ \hat{\mathbf{D}}(t, 1\ \ldots\ M)),\ 2N+2G+1+M$ values corresponding to the sliding window reference cells, including guard cells, the value in CUT and the M values from the Doppler profile for the particular range-bin.

Figure 3.1 provides an illustration of range-Doppler sliding window data interconnected with a fully connected neural network. With the first option (O1) the network is only fed the identical information as utilized by a standard SO-CFAR test while with the second option (O2) the guard cell data is also incorporated. Guard cells can potentially contain useful information for target identification due to potential range walk and range sidelobes originating from the pulse spreading function. Similarly, targets tend to spread out in Doppler, subject to the applied tapering window, and the statistical information on target impacting neighboring cells can be taken into account by a neural network. With the third option (O3), the neural network will be fed all M samples from the Doppler profile in addition to the $2N + 2G + 1$ values from the CFAR range window. The auxiliary data of O2 and O3 has always been available for detectional purposes, but it is not analytically discernible how this can be utilized to improve the target detection process; this is nevertheless a task ideally suited for neural networks who can internally construct intricate models. In all cases, the input samples to the neural network are normalized by min max normalization,

$$\hat{\mathbf{r}} = \frac{\mathbf{r} - \min(\mathbf{r})}{\max(\mathbf{r}) - \min(\mathbf{r})}. \tag{3.4}$$

The output from the last layer of the neural network, a single value output,

$$\kappa = f_{NN}(\hat{\mathbf{r}}), \tag{3.5}$$

returns a detection estimate. $f_{NN}(\hat{\mathbf{r}})$ represents the neural network modeled as a function with an input given by the normalized data $\hat{\mathbf{r}}$. A threshold test is applied on κ and if exceeded a detection is declared.

For supervised training of the proposed network we assume that a collection of L independent range-Doppler maps $\mathbf{D}_1(t, \omega), ..., \mathbf{D}_L(t, \omega)$ have been acquired wherein the targets and their positions in range and Doppler are known precisely (i.e. ground truth). A database is thereupon constructed based on realizations of CMSO-CFAR tests and window samples who lead to positive detections. A number of samples are collected for when the detection process returns a correct decision and when the detector returns a false positive. The training objective of the neural network is to distinguish between these two cases and to return either 0 or 1:

$$\hat{\kappa} = \begin{cases} 1, & \text{CMSO-CFAR: correct decision} \\ \\ 0, & \text{CMSO-CFAR: false positive,} \end{cases}$$

where $\hat{\kappa}$ is the aimed output from the neural network. This training process forces the network to evolve a statistical mechanism to separate between the two type of detections. We remark that the condition for a correct decision must also include neighboring cells if a target spreads out in range and/or Doppler due to sidelobes and if the initial detector returns a positive outcome. The objective behind the neural network training is not necessarily to retain the same P_D as for CMSO-CFAR but to exploit it to maximize the detection capability with a satisfactory low false alarm rate.

For a generic type of network training the training database should contain a wide variety of samples in order to learn to recognize different situations. This is particularly important if the network is trained on data including gap cells and/or Doppler profiles as the network can become

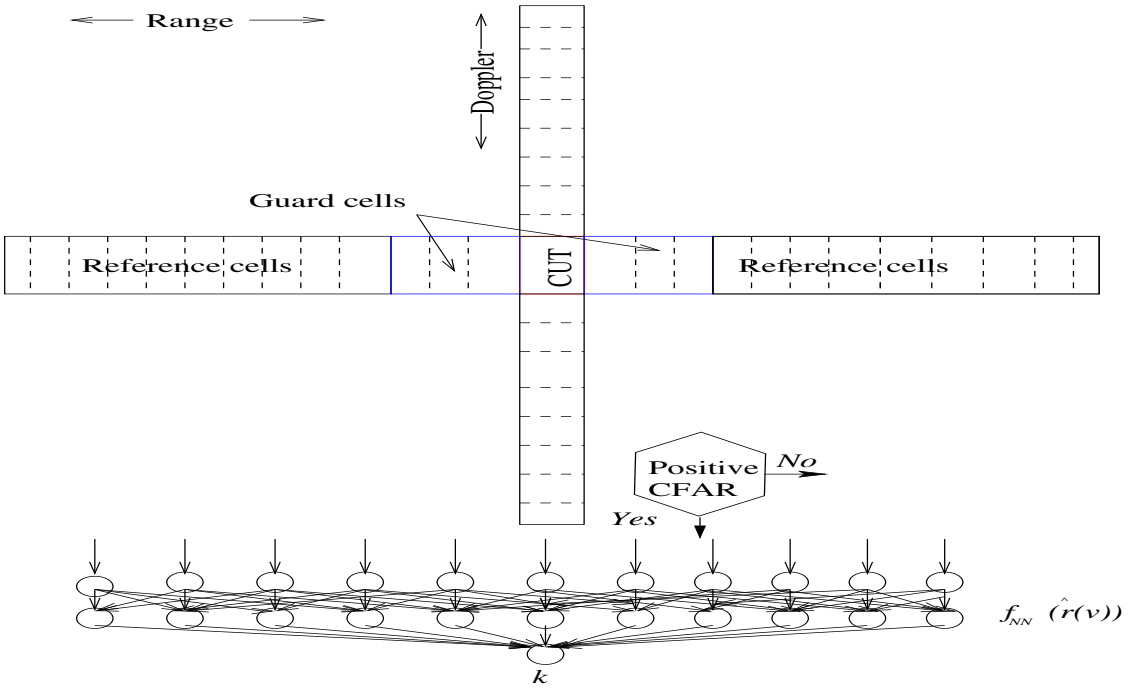

Figure 3.1 Schematic description of the detection process and data linked with a neural network.

highly specialized with respect to these inherent features. To attain better control over this, the various samples within the training database may be split into multiple categories when the initial detector returns a positive result. Possible categories for positive and correct CMSO-CFAR can be: target in noise-only environment, target in clutter region, target with the presence of another target in the reference cells, target with clutter edge on the right or left side of the reference cells and so forth. Similarly, different categories can be established for incorrect decisions, such as false positive in noise-only environment, false positive due to presence of clutter etc. A fair balance between these groups is important if the network is expected to perform equally well on all situations. In a simulated environment a good counterbalance can be achieved by making certain that the various situations all occur with equal likelihood. A neural network training based on the above criteria is in principle an optimization process with the objective to minimize the overall error of the network which can be decomposed as,

$$\min f_{NN|\hat{\mathbf{x}}} = \sum_{k=1}^{A_N} (|f_{NN}(\hat{x}_{A,k})| - 1)^2 + \sum_{k=1}^{B_N} |f_{NN}(\hat{x}_{B,k})|^2, \tag{3.6}$$

where A_N and B_N refers to the number of samples for correct or false positive detections with the sliding window samples denoted by $\hat{x}_{A,k},\ k = 1, ..., A_N$ and $\hat{x}_{B,k},\ k = 1, ..., B_N$ for the two categories.

3.3 Choice of neural network

The number of input parameters to the network will be limited between $2N + 1$ entries (O1) up to $2N + 2G + 1 + M$ values in case of O3. As the amount of input data is rather limited, we use standard fully connected feedforwarding networks for the machine learning part as these networks are able to approximate any arbitrary operator [34]. The output from a node of the network is therefore connected to every other node in the next layer. The network will consist of an input layer, an output layer with a linear transfer function and one or two hidden layers with hyperbolic tangent sigmoid activation functions. The output layer is to contain a single node as a binary detection estimate is desired. The number of hidden layers and nodes may be varied and will be discussed in the next chapter though very large networks are not desirable as they can potentially lead to overtrained networks. Contrarily, very small networks may not be able to distinguish well between true targets and false detections.

4 Illustrating examples and discussion

Neural network training is a highly data driven approach and the results will therefore depend on the type of input data and the constructed scenario. This chapter nevertheless exemplifies how the presented framework can be put to use under both noise-only and clutter oriented scenarios. In a practical setting, a radar can be set up to collect data over longer time intervals where one has accurate control over location of real targets. This can in turn be used to train networks to discriminate between true and false detections. Collected data may also be merged with simulated data based on radar properties and expected form or structure of targets. Continuous collection of data and re-training of networks can then be carried out on regular intervals to update the system and keep it up to date.

The focus of this report is on the theoretical aspects and parts of a pulsed radar system are simulated in slow-time to train neural networks under the proposed methodology and the performance is evaluated against traditional SO-CFAR and GO-CFAR detectors alongside CMSO-CFAR. The radar is assumed to transmit and receive $M = 16$ pulses with a range window of $R = 300$ range bins. In total, 11 independently fluctuating targets are modeled being placed at various range bins. The targets' reflectivity is assumed to follow a standard Swerling 1 model where the mean is varied randomly during training to mirror different power levels. The clutter shape parameter is randomly selected uniformly for each dwell to be in the range between $\nu = 0.05$ (spiky) and $\nu = 10$ (Rayleigh distributed) [35]. The clutter values are then arbitrary generated and modeled with a K-distribution function [20] to cover the first half of range bins and are additionally formed with a propagation factor to provide a dip in the clutter region. A random process additionally up or down scales the clutter to implement a greater variation in signal-to-clutter ratio from dwell-to-dwell. Noise is modeled as white Gaussian noise and to simulate noise-only scenarios, the clutter modeling aspects are discarded. For construction of the range-Doppler map the Hamming window is put to use.

We refer to figure 4.1 for an example range-Doppler map where all 11 targets stand out and are designated from A to K. In the figure, the clutter component is included and can be seen on the left side. Targets A, B, C, H, I and J can be considered to be in a clutter dominated range region and their velocities are randomly selected to be within -45 m/s to 45 m/s. For other targets, the velocity range is set between -65 m/s to 65 m/s. Targets A, C and H are within the vicinity of a clutter edge and their range placement is randomly determined to be between 0 to 9 bins to the left or right of range bins, respectively, 60 or 160 at the start and end of the second clutter region. Positive detection samples will thus experience cases of clutter edge with different distance from CUT from both sides. Targets D, E, F and I, J are closely spaced with identical velocities, but the distance amidst is randomly set between 3 to 10 range cells. With a probability of 0.5 these closely spaced targets have equal power levels while otherwise they all fluctuate randomly. Closely spaced targets are thus modeled with both matching and dissimilar reflecting values. We further remark that targets A,H, B,J and G,K are placed on the same range bin. This is important to make certain that when a network is trained on incorporating the Doppler profile (O3), then the network does not erroneously make the assumption that only a single target can be encountered on a given range-bin. The simulated scenario is set up so the different type of targets in noise-only and clutter regions, targets in clutter edges or single or closely spaced targets are accounted approximately once in a proportionally manner. The few exceptions are related to targets who occur twice in the same range-bin, such as targets G and K who are both single targets in noise-only region. All targets are moreover modeled to have a single sidelobe in range of -23dB on adjacent bins and with a probability of 0.5, range walk is simulated with a target spreading across two range-cells.

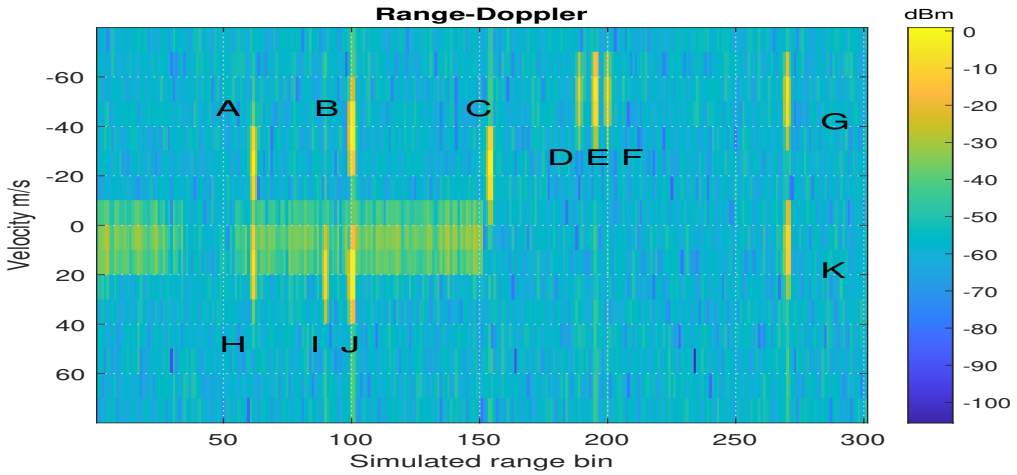

Figure 4.1 Simulated range-Doppler map

If the target is designated to spread out in range, then the neighboring cell instead determines an independent Swerling 1 value from the same distribution. Simulating target spread does not alter the performance of a standard CFAR detector with guard cells, however, a neural network can then not simply recognize a target by an expected fixed sidelobe level in bordering cells. The noise floor during simulations is also not kept fixed, rather ranges between -80 dB to -115 dB following a uniform distribution between CPIs. The variation in the above setup, particularly from dwell-to-dwell, captures a broad type of both simple and challenging detectional conditions which should be suitable for training and evaluating a generic type of detector.

After the formation of a range-Doppler map, a detection process is performed with the CFAR parameters being set as $G = 3$ guard cells and $N = 9$ averaging cells on each side with a thresholding factor of 14dB. Two values of $P = 3$ and $P = 6$ were selected for CMSO for two independent realizations of training and evaluations. To construct the training database, true and false positive detections were taken as encountered sequentially by CMSO-CFAR and new random range-Doppler maps were generated for as long as required. A total of $A_N = 100000$ positive detections were collected while the number of false positive collected detections was set to $B_N = 1000000$, resulting in 1.1 million entries for the training set. The ratio between incorrect and correct detections symbolizing the much larger number of false detections who arise with the application of CMSO-CFAR. For clutter scenarios, the number of false detections were grouped in two, half of the false detections occurring in the clutter region and the other half in the outer noise-only region. The target SNRs over all dwells ranged from -40 dB to 70 dB while the SCR varied between -60 dB to 60 dB when clutter was included.

For neural network training, all three data options were considered with two different sizes; a small $50x1$ network with one hidden layer of 50 nodes or a bigger $50x2$ network with two hidden layers The selection of 50 nodes in a layer was made as it roughly corresponds with the O3 input being set at 41 entries. For a fair comparison, the same network sizes were also kept for O2 and O1 selections. Even bigger and deeper networks were also investigated, however, the performance was found to be generally very comparable to the $50x2$ networks. Training was carried out using the scale conjugate gradient algorithm over both noise-only and clutter plus noise scenarios. The full data was put to use for training, without any division into different sets for training or validation, over a total of 1 million epochs. To inspect how training actually transfers over to detectional

performance on untrained data, a larger set of 6500 range-Doppler maps was constructed adopting the formerly described principles, but with a set mean power value for the targets. Each map was evaluated in full through different detection methods and the trained neural networks to build up statistics. This process was repeated with varying average target power levels to obtain P_D and P_{FA} curves with respect to mean target SNR or SCR. P_D was calculated as the number of correctly detected targets relative to the total number of simulated targets while P_{FA} as the number of incorrectly detected targets in relation to total number of tests (26.2 millions per SNR/SCR). The network threshold was fixed at $\kappa > 0.8$ which represents an outcome with high degree of certainty. Other values of κ can be chosen to shift the curves up or downwards [29].

Data option and network size	$P = 3$	$P = 6$
O1, $50x1$	0.012815	0.010665
O2, $50x1$	0.004880	0.003529
O3, $50x1$	0.001576	0.001104
O1, $50x2$	0.009597	0.006641
O2, $50x2$	0.002912	0.001334
O3, $50x2$	0.000273	0.000031

Table 4.1 Neural network training errors, noise-only training

4.1 Noise-only scenario

If a sensor operates mainly in a homogeneous environment, then the described clutter modeling aspects can be eliminated to detect single and dense targets in noise. Training on only noise provides opportunity to understand the behavior of neural networks and the classification process in a simpler context. Later, the performance can be compared against a network trained on both noise and clutter. The network convergence error rates after a completed training process are given in table 4.1 for the noise-only case. Training over O2 dataset gives several times improvement over O1 while a further enhancement is attainable by using O3. The error rates for $P = 6$ are lower than for $P = 3$ pointing towards the fact that a low selection of P can result in a very large number of incorrect detections who are more difficult to classify. Two layer networks generally yield lower error rates though the improvement could stem from either the ability to detect more targets correctly or identify more false detections.

Subsequent training, results from the evaluation process executed over the untrained dataset of range-Doppler maps are given in figures 4.2 and 4.3 where the top plot depicts the P_D curves while the P_{FA} curves are on the lower plot. The x-axis follows the average SNR in dB with fluctuating Swerling 1 targets. We remark that the P_D values are quite low, even at high average SNR, as the scenario shown in figure 4.1 is quite demanding and none of the detection methods can provide fully satisfactory outcomes for detecting multiple closely spaced target and targets embedded in clutter. The random fluctuation in SNR makes it even harder to obtain high detection rates. Nevertheless, the best P_D performance stems from CMSO-CFAR (dashed magenta) which also yields the highest P_{FA}. At the other extreme, GO-CFAR (magenta with diamonds) gives the lowest false alarm rate at the expense of lowest detectional capability. The standard SO-CFAR (solid black) performs in-between these two extreme detectors. Results of classification of CMSO-CFAR detections from the neural network trained only on references cells (O1) for $50x1$ (blue starred) shows a very close

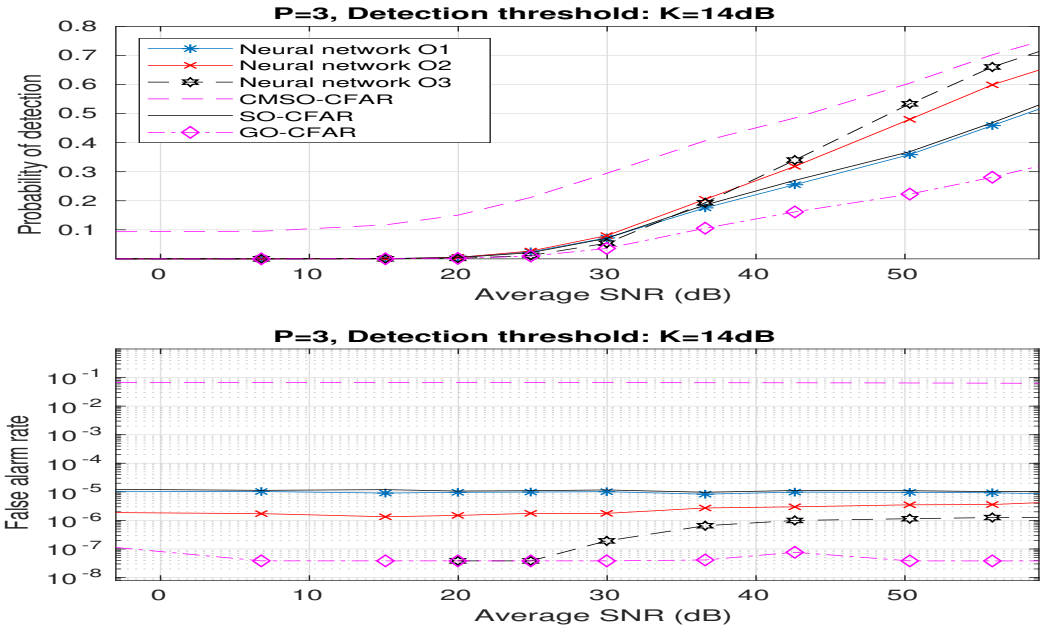

Figure 4.2 P_D and P_{FA}, Noise-only scenario, 50x1 network, $P = 3$

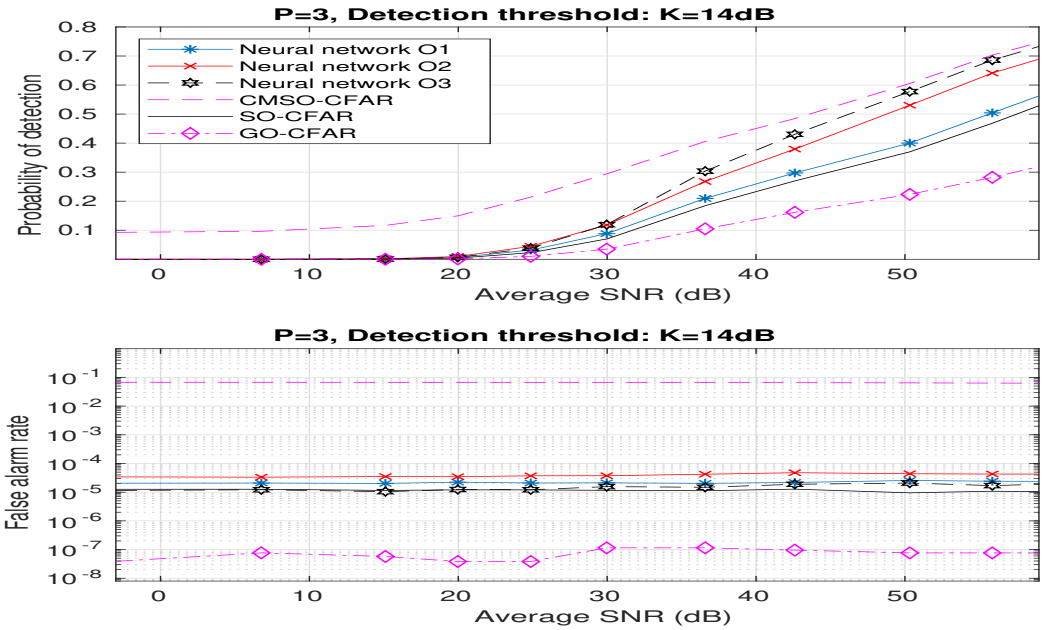

Figure 4.3 P_D and P_{FA}, Noise-only scenario, 50x2 network, $P = 3$

convergence towards standard SO-CFAR for both P_D and P_{FA}. Although this solution does not lead to the detection of more than two closely spaced targets, it still becomes the best fit for the dataset and demonstrates the network's ability to coincide towards a classical solution if no alternatives can be found.

The other networks in figure 4.2, who utilize the guard cells information (O2, red) or guard cells combined with Doppler profile (O3, black starred), provide a clear P_D advantage over standard SO-CFAR and at high SNR the curves can be seen converging towards CMSO-CFAR. The false alarm rate is well below CMSO- or SO-CFAR though remains above GO-CFAR. This validates the basic claim that there is useful information present in guard cells and the Doppler cells. The false alarm rate for the case of O3 $50x1$ trained neural network stands out as it does not follow the CFAR property but rather behaves in an adaptive manner. At low SNR the P_{FA} performance is more similar to GO-CFAR but attains a higher floor level at bigger SNRs. Otherwise, comparing the smaller $50x1$ networks with the deeper $50x2$ networks (figure 4.3), one notices that the P_D is always better with the bigger networks though the false alarm rates are higher. The P_D for the O1 $50x2$ network is marginally better than SO-CFAR but progresses with data options of O2 and O3. For $50x2$ cases, the P_{FA} fluctuates around that of SO-CFAR. Although these networks evaluate positive detections coming from a CMSO-CFAR detector, all of these are clearly approximating a SO-CFAR type of detectional approach and revising it based on available extra information. With O3 it is possible to attain CMSO-CFAR detectional level for high SNR targets but the choice of O2 is also quite beneficial as an overall improvement on the traditional SO-CFAR detector. Recognizing and detecting a target correctly, compared to labeling it as a false detection, is evidently a more demanding task and must be based on potential information only available in the CUT, the few guard cells and/or the Doppler cells adjacent to the CUT.

The selection of $P = 3$ is useful for obtaining a high probability of detection but the false alarm rates, except for the single case of $50x1$ O3, remain relative large compared to GO-CFAR. To further curtail the P_{FA} a greater value of P can be practiced which will reduce the P_D but still be able to handle many complex situations. For the training and evaluation process with $P = 6$ the results are depicted in figures 4.4 and 4.5.

As one would predict, advancing from $P = 3$ to $P = 6$ reduces the detection capability of CMSO-CFAR, however, the reduction is quite small at medium to high SNR values. At low SNR the fixed detection capability, which can be attributed to randomness, is now eliminated. To some extent, the results mirror the previous cases of $P = 3$ but with a decreased false alarm rate, particularly for the smaller networks of $50x1$ (figure 4.4) who are now closer to the GO-CFAR level. In case of O1, the P_D and P_{FA} are both lower than SO-CFAR but with same curve characteristic for P_D; this solution is thus similar to a traditional SO-CFAR detector where a different trade-off is being made between P_D and P_{FA}. The use of O2 (red curve) gives a comparable P_D as of SO-CFAR with a low false alarm error closer to GO-CFAR. The application of O3 (black starred) gives an even more reduced $P_{FA} < 1 \cdot 10^{-8}$ though the detection capability at medium SNR values is also hampered. Using Doppler information the network manages to identify false detections well and the training weighting is such that a reduction in P_{FA} is preferred over P_D. For the bigger networks of $50x2$ (figure 4.5) the false alarm rates are not as low, but are distributed around $1 \cdot 10^{-6}$, doing better than both CMSO or SO-CFAR, with the O3 method having a slight advantage. That a neural network trained only on noise and utilizing the same limited information (O1) as of a traditional CFAR detector can offer roughly identical P_D performance as SO-CFAR but with a lower false alarm rate is an important finding here and is discussed further in chapter 4.3.

Reviewing the results on noise-only setup, we observe that for the proposed training strategy,

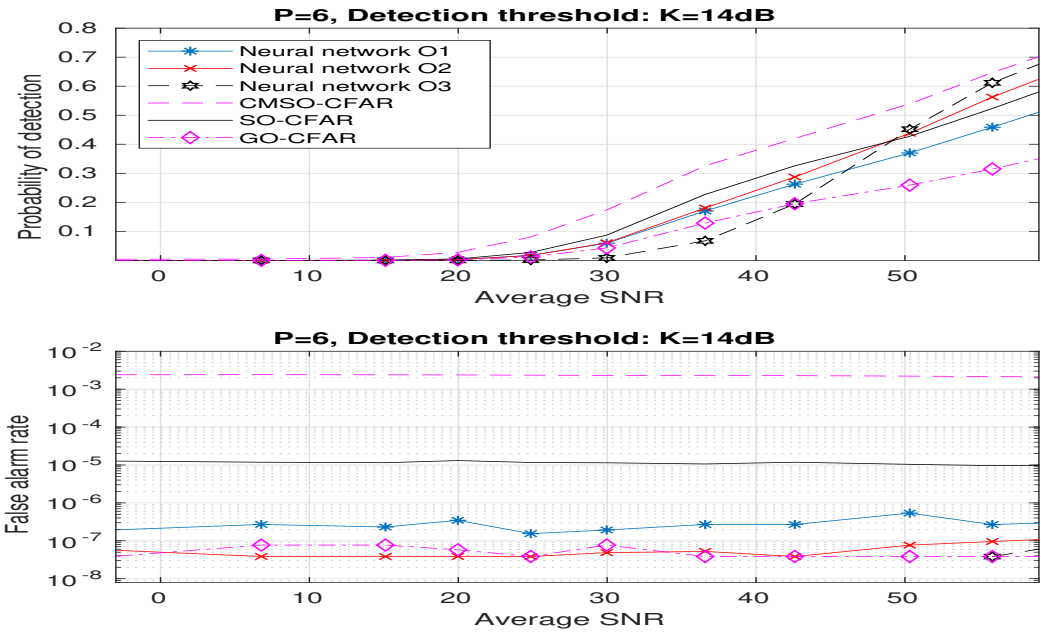

Figure 4.4 P_D *and* P_{FA}*, Noise-only scenario,* $50x1$ *network,* $P = 6$

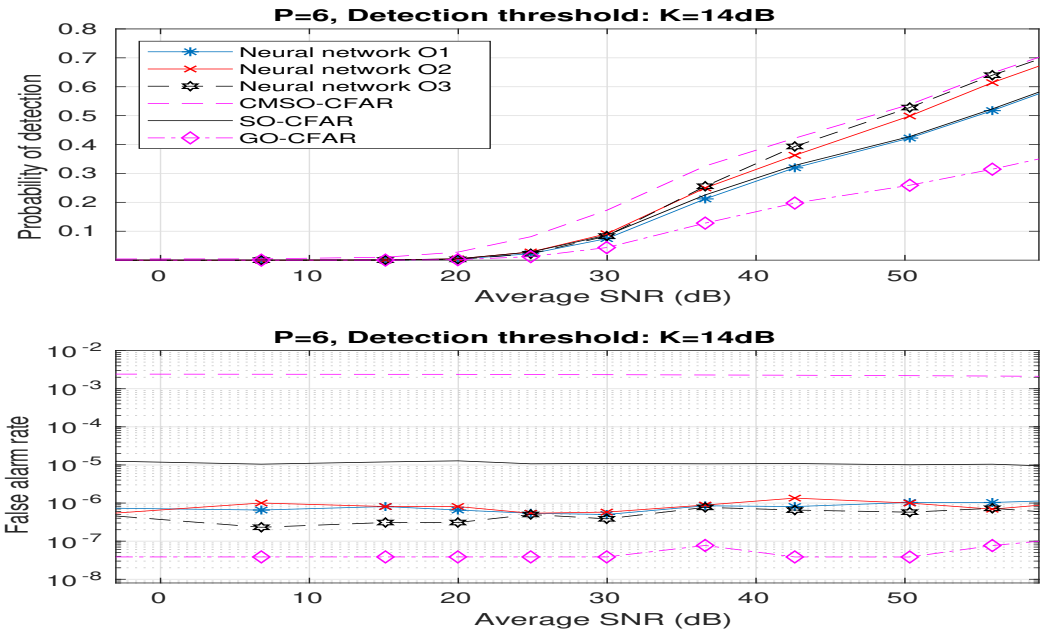

Figure 4.5 P_D *and* P_{FA}*, Noise-only scenario,* $50x2$ *network,* $P = 6$

even small sized networks are very capable of identifying and reducing the number of false detections even though the starting premise may be a very coarse CMSO-CFAR detector. The detectional performance is nevertheless strongly dependent upon how much data the network is fed. Deeper

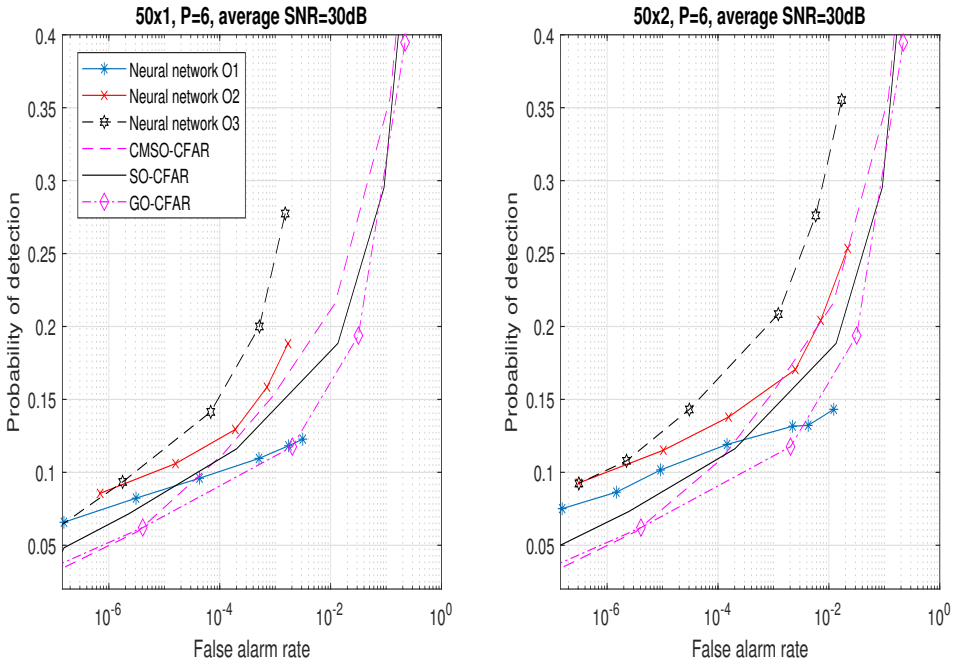

Figure 4.6 Receiver operating characteristic curves, noise-only scenario

networks manage to reduce the number of incorrect detections though they tend to place greater emphasis on the detectional aspects and, regardless the data option, end up offering a very similar false alarm rate. This explains the results of [21, 22] as the improvements demonstrated there can now be linked to the application of the O2 method. If no adjoining cell information is provided then the trained network may converge to a standard solution (as shown for $P = 3$), while a lower false alarm can still be achieved if the initial detector is more restrained (as demonstrated for $P = 6$).

The assertion for training of a neural network commences from a fixed detection threshold. This is in contrast to a traditional setup, where a desired P_{FA} is first determined and then one aims to maximize the P_D. By varying the threshold level K and training multiple networks, keeping other parameters fixed, receiver operating characteristic (ROC) curves can still be generated where P_D and P_{FA} numbers can be compared against each others. Figure 4.6 provides an example of such curves over the defined scenario for medium average SNR with $P = 6$ and both $50x1$ and $50x2$ networks, complementing figures 4.4 and 4.5.

As the curves demonstrate, the O3 data option provides the leading P_D/P_{FA} ratios in both cases. The deeper network (right) can deliver higher quotients, noticeably at lower P_{FA} levels whereas the $50x1$ network (left) starts off at a smaller P_{FA} as it is more fruitful in reducing false detection when there are many of these. O2 is also able to yield outcomes better than both GO or SO-CFAR though there are certain intervals where the effectiveness of the $50x2$ network can be similar to the CMSO-CFAR detector; a trait the smaller network does not exhibit. The O1 selection is most applicable at medium to high P_{FA} levels, i.e. when the number of false detections from the initial detector is small then the network can distinguish between the two classes with an advantage and follows or exceeds the performance of traditional detectors. The choice between $50x1$ or $50x2$ then depends primarily upon the aimed P_{FA}. The presence of multiple closely spaced targets makes it difficult to obtain a high P_D as observed in previous figures, however, the curves demonstrate how

different amount of data can be utilized by a neural network for leverage while the initial detector may remain oblivious to it.

4.2 Clutter scenario

The preceding section established some important reference points for neural network target detection in noise-only surroundings. In a more convoluted environment with the presence of sea or ground clutter, target detection becomes more difficult, however, the use of CMSO-CFAR is a viable option as it can offer a high detection capability though with an inflated false alarm rate. We do note that false detections arising from clutter are likely to exhibit certain properties and have a statistical structure which a neural network may be able to recognize with more ease than false detections stemming from noise. The convergence error rates after the training session, for the combined case of noise and clutter setup, as of figure 4.1, are provided in table 4.2. The error level decreases as the network engages with more data and as P and the size of the network is increased, nonetheless, the networks do not adapt to the data as well as for the noise-only case (table 4.1).

Data option and network size	$P = 3$	$P = 6$
O1, $50x1$	0.020144	0.017909
O2, $50x1$	0.008889	0.007103
O3, $50x1$	0.006807	0.003588
O1, $50x2$	0.015442	0.012543
O2, $50x2$	0.006807	0.004495
O3, $50x2$	0.004720	0.000991

Table 4.2 Neural network training errors, clutter and noise

From the table, one may conclude that a bigger network and more input data is most appropriate options for a neural network training, but to determine the impact on P_D and P_{FA} simulations need to be carried out on an untrained data set as outlined previously but now with incorporated clutter. The results from subsequent evaluation for the case of $P = 3$ and $50x1$ network are given in figure 4.7 while figure 4.8 demonstrates the use of larger $50x2$ networks. The lower x-axis provides the average SNR of the targets in noise-only region while the average SCR for the targets in the clutter region is given in the upper x-axis, the resulting signal to noise plus clutter ratio being in the interval from -21dB to 40dB.

Introducing clutter in the first half of the range-Doppler map lowers the detection capability a little, however, the major impact is on the false alarm rates for CMSO-CFAR and SO-CFAR who are now much higher. The trained $50x1$ networks (figure 4.7) reduce the false alarm rates substantially though this also comes with a large reduction in the P_Ds. Only at high SNR/SCR the detection rates for O2 and O3 exceed standard SO-CFAR, otherwise the P_D remains below SO-CFAR. Even though the starting point is a CMSO-CFAR detector, the O1 method is particularly only interesting as a GO-CFAR replacement since it does better than GO-CFAR with respect to detection while the P_{FA} remains similar to GO-CFAR. The deeper $50x2$ networks (figure 4.8) are much more successful in P_D efficiency which is well above that of SO-CFAR depending on whether O2 or O3 method is used while the false alarm rates are all comparable to GO-CFAR. The case of O1 is an exception as the detection capability is just beneath SO-CFAR though the P_{FA} is significantly lower. As the false alarm rates for O1 and O2 are similar across $50x1$ and $50x2$ one

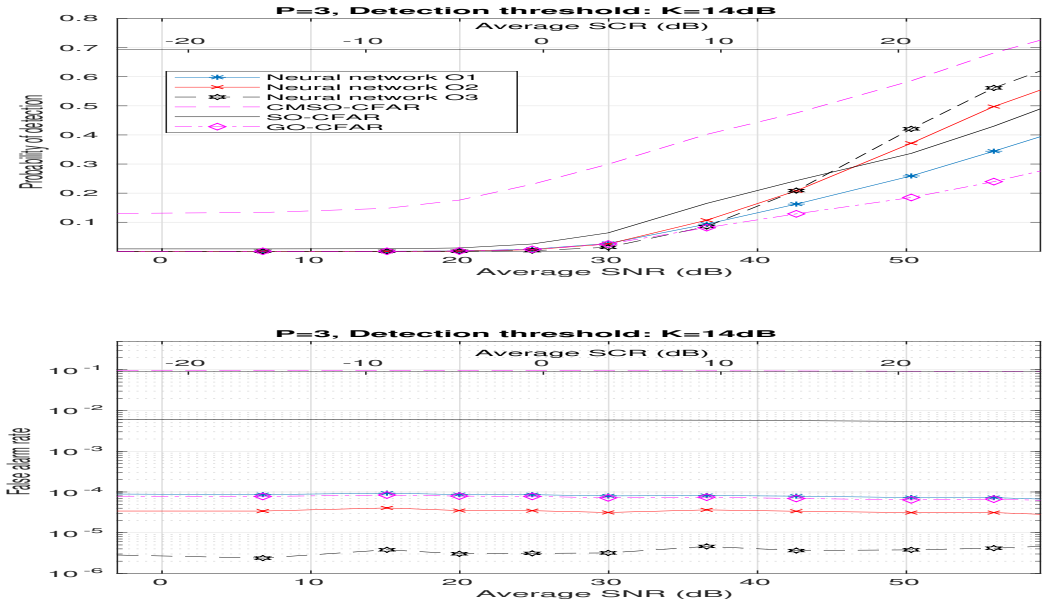

Figure 4.7 P_D *and* P_{FA}*, Clutter and noise scenario,* $50x1$ *network,* $P = 3$

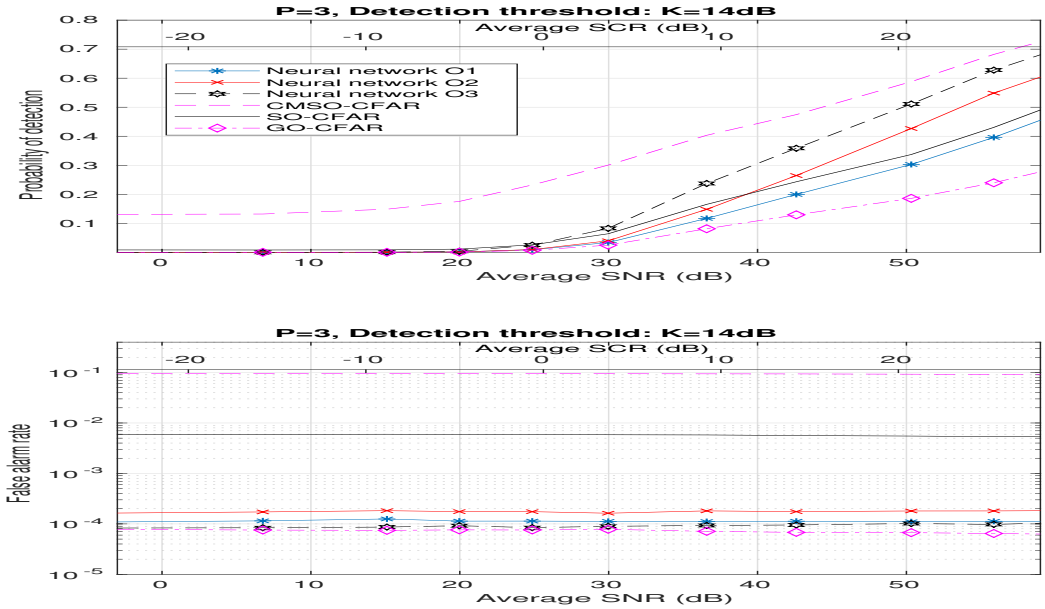

Figure 4.8 P_D *and* P_{FA}*, Clutter and noise scenario,* $50x2$ *network,* $P = 3$

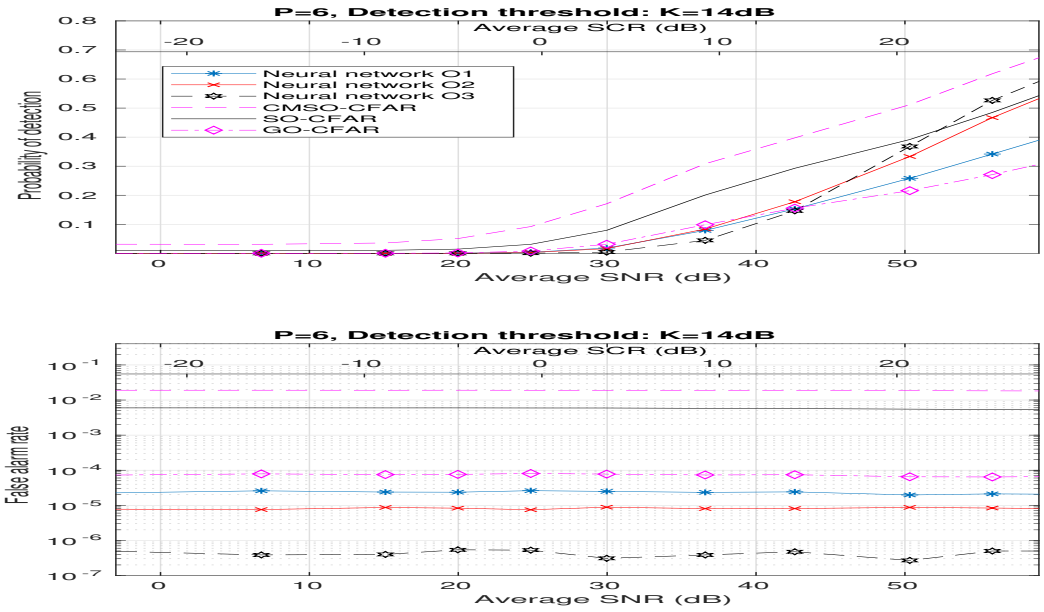

Figure 4.9 P_D and P_{FA}, Clutter and noise scenario, 50x1 network, $P = 6$

can conclude that the smaller networks lack necessary resources to positively discriminate between the various type of targets in complicated environments.

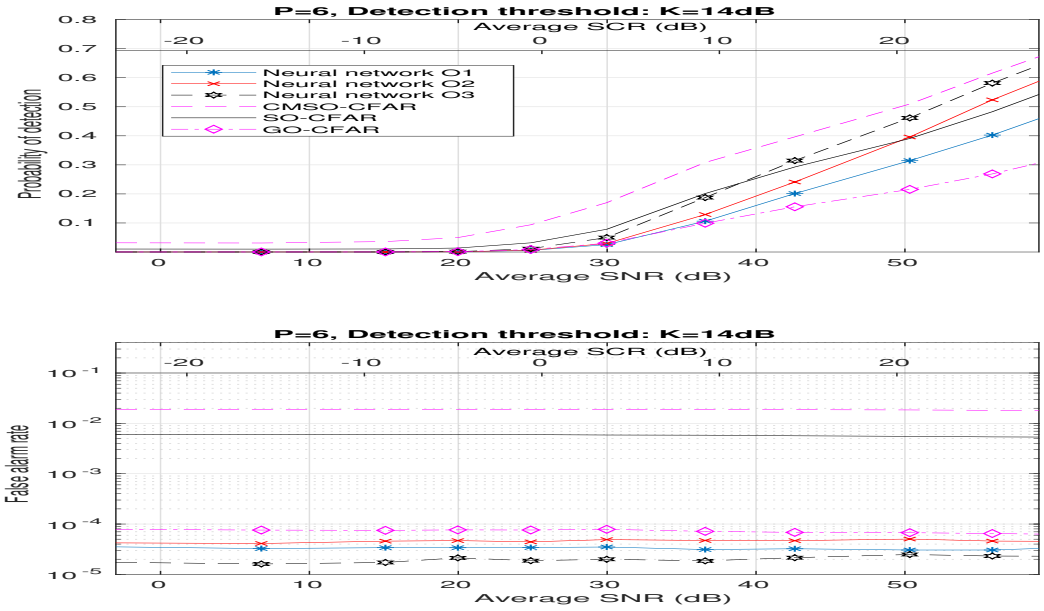

Figure 4.10 P_D and P_{FA}, Clutter and noise scenario, 50x2 network, $P = 6$

The choice of $P = 3$ is a challenging situation and the results from $P = 6$ are given in figures 4.9 and 4.10. The smaller $50x1$ networks are, as in the previous case, able to reduce the false alarm rates greatly but with a marked decrease in the detection capability which is only on par with GO-CFAR at low to medium SNRs. At high SNR/SCR levels the performance approaches that of SO-CFAR with either O2 or O3. The deeper $50x2$ networks of figure 4.10 yield better outcomes and although the reduction in the average P_{FA} is lower it is still significantly curtailed from the original CMSO- or SO-CFAR and float around that of GO-CFAR. The detection rates are all between SO-CFAR and CMSO-CFAR where the highest detection capability arises from O3 with a couple of dB reduction if O2 is employed. Both of these methods exhibit the same curve gradient as of CMSO-CFAR. The O1 method also performs better with $50x2$ compared to $50x1$ although the P_D remains suboptimal against standard SO-CFAR.

The provided figures have established some capabilities of trained neural networks for binary classification. The P_{FA} as shown in all the figures is essentially constant satisfying the CFAR property at both low and high SNR regimes. The only exception being the case of O3 training and the smaller $50x1$ network for $P = 3$ where the small choice of P leads to very coarse estimation of the noise level, as expected.

To consolidate figure 4.10, figure 4.11 displays two ROC curves for $P = 6$ and $50x2$ networks trained for different thresholds for two different SNR and SCR settings. Not all combinations of P_D/P_{FA} are achievable as trained networks will always try to lower the initial false alarm rate. The best gain is recovered from the combined CMSO-CFAR and neural network detector with O3 data strategy while O2 also surpasses the traditional detectors. The O2 method for the low SCR plot on the left side exhibits an adaptive behavior where it converges towards standard GO-CFAR as the P_{FA} increases. Identical to the noise-only case of figure 4.6, O1 can result in improved outcomes but only at higher P_{FA} values which shows the importance of the sidelobe information present in guard cells and Doppler.

4.3 Characteristic evaluation

The curves in the depicted plots demonstrate the average performance of the trained networks for the defined scenario at various SNR/SCR levels. To further investigate how these networks would perform for specific target conditions more detailed evaluations were carried out for $P = 6$. Four different simulated setups were considered. Table 4.3 provides the numerical outcomes for the first two situations with only a single (S) target (target C in figure 4.1) in noise-only environment or only three multiple (M) close targets (D, E and F) in noise-only environment. In table 4.4 the results are given for the cases with detection in mixed noise and clutter environment with either only a single (S) target in clutter edge (target C) or only dual multiple (M) targets in clutter region (targets I and J). Notice that this therefore becomes an overall simpler evaluation scenario with emphasis on only either a single target or multiple closely spaced targets. One can therefore expect high detection probability for the single target case, even from traditional methods; while the second (M) case will be more challenging. The tables in all cases provide the mean detectional and false alarm rates over varying SNR as described for the training stage, evaluated across 300 untrained range-Doppler maps with approximately 103 million CFAR tests. A 0 in the table refers to a $P_{FA} < 9 \cdot 10^{-9}$ and the three bottom rows represent the fallout from traditional CFAR detection schemes.

The tables confirm the plots in establishing the progression in P_D as one moves from feeding less data to more data i.e. from O1 to O3. Comparing the networks trained on noise-only mode against those trained on noise and clutter (top six rows against six bottom NN rows for both tables),

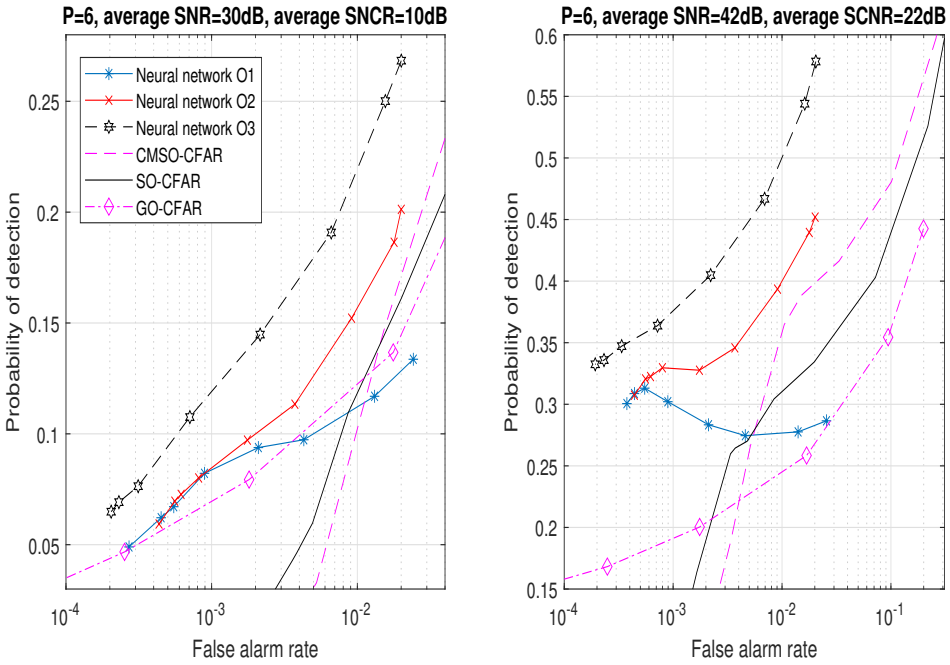

Figure 4.11 Receiver operating characteristic curves, clutter and noise scenario

Detector (trained on)	S: P_D	S: P_{FA}	M: P_D	M: P_{FA}
NN (N) O1, 50x1	0.76	$5.78\cdot10^{-8}$	0.34	$3.92\cdot10^{-8}$
NN (N) O2, 50x1	0.80	$5.78\cdot10^{-8}$	0.51	$1.96\cdot10^{-8}$
NN (N) O3, 50x1	0.82	$9.64\cdot10^{-9}$	0.78	0
NN (N) O1, 50x2	0.76	$7.52\cdot10^{-7}$	0.64	$4.61\cdot10^{-7}$
NN (N) O2, 50x2	0.81	$8.67\cdot10^{-7}$	0.77	$3.92\cdot10^{-7}$
NN (N) O3, 50x2	0.82	$3.95\cdot10^{-7}$	0.80	$1.07\cdot10^{-7}$
NN (N+C) O1, 50x1	0.70	0	0.41	$9.81\cdot10^{-9}$
NN (N+C) O2, 50x1	0.79	0	0.63	0
NN (N+C) O3, 50x1	0.79	$1.92\cdot10^{-8}$	0.70	$9.64\cdot10^{-9}$
NN (N+C) O1, 50x2	0.72	$2.89\cdot10^{-8}$	0.60	$2.35\cdot10^{-7}$
NN (N+C) O2, 50x2	0.79	$2.89\cdot10^{-8}$	0.75	$2.02\cdot10^{-7}$
NN (N+C) O3, 50x2	0.82	$5.01\cdot10^{-7}$	0.79	$5.11\cdot10^{-7}$
CMSO-CFAR	0.82	$2.43\cdot10^{-3}$	0.82	$2.38\cdot10^{-3}$
SO-CFAR	0.77	$1.19\cdot10^{-5}$	0.62	$1.10\cdot10^{-5}$
GO-CFAR	0.74	$3.85\cdot10^{-8}$	0.09	$1.96\cdot10^{-8}$

Table 4.3 Performance comparison, single target (S) and multiple close targets (M) in noise, P=6

those trained on noise-only yield foremost performance in clutter free environments. When the networks trained on only noise are evaluated in clutter surroundings (top 6 rows of table 4.4) then the comparable P_{FA} increases, up to to the level of SO-CFAR. This is still better than that of

Detector (trained on)	S: P_D	S: P_{FA}	M: P_D	M: P_{FA}
NN (N) O1, 50x1	0.61	$2.92\cdot10^{-4}$	0.39	$4.00\cdot10^{-4}$
NN (N) O2, 50x1	0.78	$1.89\cdot10^{-4}$	0.65	$1.95\cdot10^{-4}$
NN (N) O3, 50x1	0.81	$3.77\cdot10^{-3}$	0.69	$3.76\cdot10^{-3}$
NN (N) O1, 50x2	0.72	$1.17\cdot10^{-3}$	0.62	$1.47\cdot10^{-3}$
NN (N) O2, 50x2	0.80	$1.62\cdot10^{-3}$	0.70	$1.76\cdot10^{-3}$
NN (N) O3, 50x2	0.82	$9.04\cdot10^{-3}$	0.73	$9.20\cdot10^{-3}$
NN (N+C) O1, 50x1	0.61	$2.51\cdot10^{-5}$	0.41	$2.38\cdot10^{-5}$
NN (N+C) O2, 50x1	0.76	$8.59\cdot10^{-6}$	0.62	$8.40\cdot10^{-6}$
NN (N+C) O3, 50x1	0.77	$4.04\cdot10^{-7}$	0.66	$4.86\cdot10^{-7}$
NN (N+C) O1, 50x2	0.66	$3.45\cdot10^{-5}$	0.58	$3.31\cdot10^{-5}$
NN (N+C) O2, 50x2	0.79	$4.80\cdot10^{-5}$	0.68	$4.73\cdot10^{-5}$
NN (N+C) O3, 50x2	0.81	$1.98\cdot10^{-5}$	0.71	$1.99\cdot10^{-5}$
CMSO-CFAR	0.82	$1.89\cdot10^{-2}$	0.74	$1.90\cdot10^{-2}$
SO-CFAR	0.77	$9.00\cdot10^{-3}$	0.66	$3.85\cdot10^{-3}$
GO-CFAR	0.60	$7.63\cdot10^{-5}$	0.14	$7.03\cdot10^{-5}$

Table 4.4 Performance comparison, single target in clutter edge (S) and multiple targets in clutter (M), P=6

CMSO-CFAR considering the fact that these networks have not been provided any clutter data for training. Networks trained on both noise and clutter (6 bottom NN rows in both tables) offer low P_{FA} regardless scenario, however, also yield a reduced P_D when executed on noise-only setups. The loss is then more significant in case of O1 compared to O3, for example, comparing row 4 with row 10 a P_D reduction can be seen of 4%-6%, while for O3, row 6 against row 12, the disadvantage is of 0%-2%. Networks trained on a combination of backgrounds thus exhibit a loss against more specialized networks, but this can to some extend be mitigated by a training process based on more input information. As established in the previous sections, employing single layer 50x1 networks generally yield lower P_{FA} compared to a 50x2 network, at the expense of P_D. Nevertheless, by training on both noise and clutter and employing a 50x2 neural network with O2 or O3 data strategy (row 11 and 12) one can obtain a P_D which for all evaluated cases in the tables is higher than the one of SO-CFAR while the false alarm rates are more comparable to GO-CFAR in clutter based scenarios and just marginally higher in noise-only conditions.

The networks trained in a noise-only mode notably provide exceptional good noise limited detection (top 6 rows of table 4.3). The P_D performance is as good as SO-CFAR while the P_{FA} is at the levels of GO-CFAR. The exceptions to this are related to the smaller 50x1 O1 neural networks trained on noise-only (row 1) or noise and clutter (row 7) in both tables. The single target P_D is closer to GO-CFAR and these two smaller networks clearly sacrifice the P_D performance of multiple targets in order to yield an overall lower false alarm rate. This strategy, on average, works well for the considered scenario taking account of limited capacity of the neural network. The bigger 50x2 O1 networks (row 4 and row 10) balance out this much better and can detect dense targets with more ease.

The 50x2 O1 network (row 4 in table 4.3) is not using any more information than standard SO-CFAR and decreases the P_D by 1%, but with a marked lower P_{FA} demonstrating that certain types of false detections can systematically be curtailed by only utilizing the reference cell information. To

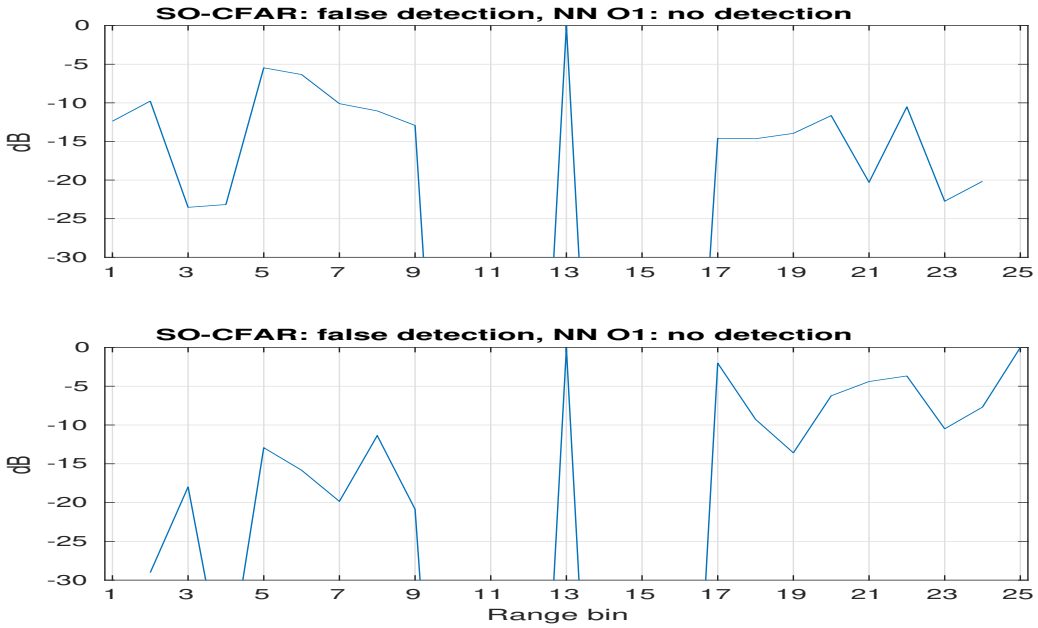

Figure 4.12 Two sliding window examples with incorrect SO-CFAR detection but correct NN classification

visually illustrate this, figure 4.12 shows two randomly collected examples of sliding window data where traditional CMSO/SO-CFAR detectors generate a false positive while the network classifies both detections as false. In both cases the ratio between the CUT and noise floor is marginally satisfied and the only reason why SO-CFAR returns a positive detection is due to the presence of a few dips who aid in satisfying the detectional criteria. These type of situations can be analyzed and later taken into consideration by a neural network during the evaluation process.

5 Final remarks

This report presented an implementation of artificial neural networks to identify between true and false detections. It was suggested to utilize a modified version of SO-CFAR to increase the number of detections while also augmenting the false alarm rate. The objective of the on-following neural network is to only study positive detections and reduce the false alarm rate to an acceptable low level. Various strategies on how a neural network training can be accomplished were investigated in detail and it was shown that a reduction of false alarm can typically be made with only moderate loss in the probability of detection with respect to traditional CFAR detectors. In this regard, incorporating the guard cell or the Doppler profile information is highly constructive for a neural network assuming that the target and environmental specifications can be taken into account. Different trade-offs can be achieved by adjusting parameters where smaller fully connected feedforwarding connected networks are particularly well-suited for significant reduction of false alarm rates while deeper networks tend to show a greater emphasis towards target detection. By altering the various parameters and e.g. the ratio between correct and false detections different type of networks can easily be constructed to satisfy specific needs of given scenarios.

References

[1] J. Akhtar, "A neural network framework for binary classification of radar detections," *EURASIP Journal on Advances in Signal Processing*, no. 90, 2021.

[2] G. V. Trunk, "Range resolution of targets using automatic detectors," *IEEE Transactions on Aerospace and Electronic Systems*, vol. 14, no. 5, pp. 750–755, 1978.

[3] M. Weiss, "Analysis of some modified cell-averaging CFAR processors in multiple-target situations," *IEEE Transactions on Aerospace and Electronic Systems*, vol. 18, pp. 102–114, Jan. 1982.

[4] H. Rohling, "Radar CFAR thresholding in clutter and multiple target situations," *IEEE Transactions on Aerospace and Electronic Systems*, vol. 19, no. 4, pp. 608–621, 1983.

[5] V. Anastassopoulos and G. Lampropoulos, "Optimal CFAR detection in Weibull clutter," *IEEE Transactions on Aerospace and Electronic Systems*, vol. 31, pp. 52–64, Jan. 1995.

[6] S. Watts, "Cell-averaging CFAR gain in spatially correlated K-distributed clutter," *IET Radar, Sonar & Navigation*, vol. 143, pp. 321–327, Oct. 1996.

[7] S. Erfanian and V. T. Vakili, "Introducing switching ordered statistic CFAR type i in different radar environments," *EURASIP Journal on Advances in Signal Processing*, no. 525704, 2009.

[8] O. B. Daho, J. Khamlichi, O. Chappe, B. Lescalier, A. Gaugue, and M. Menard, "Using CFAR algorithm to further improve a combined through-wall imaging method," in *European Signal Processing Conference*, pp. 2521–2525, 2012.

[9] G. V. Weinberg, "Coherent CFAR detection in compound gaussian clutter with inverse gamma texture," *EURASIP Journal on Advances in Signal Processing*, no. 105, 2013.

[10] F. Gini and M. Greco, "Suboptimum approach to adaptive coherent radar detection in compound-gaussian clutter," *IEEE Trans. Aerospace and Electronic Systems*, vol. 35, pp. 1095–1104, July 1999.

[11] Y. Abramovich and O. Besson, "On the expected likelihood approach for assessment of regularization covariance matrix," *IEEE Signal Processing Letters*, vol. 22, pp. 777–781, 2015.

[12] E. Aboutanios and L. Rosenberg, "Single snapshot coherent detection in sea clutter," in *IEEE Radar Conference*, 2019.

[13] J. Liu, D. Massaro, D. Orlando, and A. Farina, "Radar adaptive detection architectures for heterogeneous environments," *IEEE Trans. Signal Processing*, vol. 68, pp. 4307–4319, July 2020.

[14] S. Yan, F. Lotfi, S. Chen, C. Hao, and D. Orlando, "Innovative two-stage radar detection architectures in adverse scenarios using two training data sets," *IEEE Signal Processing Letters*, vol. 28, 2021.

[15] D. Xu, P. Addabbo, C. Hao, J. Liu, D. Orlando, and A. Farina, "Adaptive strategies for clutter edge detection in radar," *Signal Processing*, vol. 186, Sept. 2021.

[16] F. Amoozegar and M. Sundareshan, "A robust neural network scheme for constant false alarm rate processing for target detection in clutter environment," in *Proc. American Control Conference*, 1994.

[17] P. P. Gandhi and V. Ramamurti, "Neural networks for signal detection in non-gaussian noise," *IEEE Trans. Signal Processing*, vol. 45, pp. 2846–2851, Nov. 1997.

[18] G. López-Risueño, J. Grajal, S. Haykin, and R. Díaz-Oliver, "Convolutional neural networks for radar detection," in *Internation Conference on Artificial Neural Networks*, pp. 1150–1155, 2002.

[19] N. Galvez, J. Pasciaroni, O. Agamennoni, and J. Cousseau, "Radar signal detector implemented with artificial neural networks," in *Proc. XIX Congreso Argentino de Control Automatico*, 2004.

[20] K. Cheikh and F. Soltani, "Application of neural networks to radar signal detection in K-distributed clutter," *IET Radar, Sonar & Navigation*, vol. 153, pp. 460–466, Oct. 2006.

[21] J. Akhtar and K. E. Olsen, "A neural network target detector with partial CA-CFAR supervised training," in *Proc. of International Conference on Radar*, 2018.

[22] J. Akhtar and K. E. Olsen, "GO-CFAR trained neural network target detectors," in *Proc. of IEEE Radar Conference*, 2019.

[23] J. T. L. Wang and Q. Liao, "A study on radar target detection based on deep neural networks," *IEEE Sensors Letters*, vol. 3, March 2019.

[24] M. Carretero, R. Harmanny, and R. Trommel, "Smart-CFAR, a machine learning approach to floating level detection in radar," in *Proc. 16th European Radar Conference*, 2019.

[25] S. Wagner and W. Johannes, "Target detection using autoencoders in a radar surveillance system," in *Proc. of Intl. Radar Conference*, 2019.

[26] W. Ng, G. Wang, S., Z. Lin, and B. Dutta, "Range-Doppler detection in automotive radar with deep learning," in *Proc. International Joint Conference on Neural Networks*, 2020.

[27] D. Gusland, S. Rolfsjord, and B. Torvik, "Deep temporal detection - a machine learning approach to multiple-dwell target detection," in *Proc. of IEEE Radar Conference*, 2020.

[28] A. Bhattacharya and R. Vaugha, "Deep learning radar design for breathing and fall detection," *IEEE Sensors Journal*, vol. 20, pp. 5072–5085, May 2020.

[29] J. Akhtar, "Training of neural network target detectors mentored by SO-CFAR," in *European Signal Processing Conference*, pp. 1522–1526, 2020.

[30] P. P. Gandhi and S. A. Kassam, "Optimality of the cell averaging CFAR detector," *IEEE Trans. Inf. Theory*, vol. 40, pp. 1226–1228, Nov. 1994.

[31] J. T. Rickard and G. M. Dillard, "Adaptive detection algorithms for multiple-target situations," *IEEE Transactions on Aerospace and Electronic Systems*, vol. 13, no. 4, pp. 338–343, 1977.

[32] S. Himonas and M. Barkat, “Automatic censored CFAR detection for nonhomogeneous environments,” *IEEE Transactions on Aerospace and Electronic Systems*, vol. 28, pp. 286–304, Jan. 1992.

[33] M. Mashade, “Analysis of the censored-mean level CFAR processor in multiple target and nonuniform clutter,” *IEE Proceedings - Radar, Sonar and Navigation*, vol. 142, pp. 259–266, Oct. 1995.

[34] H. Huttunen, *"Deep neural networks: A signal processing perspective"*. Handbook of Signal Processing Systems (Third Edition), S. S. Bhattacharyya, E. F. Deprettere, R. Leupers, and J. Takala, Eds. Springer, 2019.

[35] M. M. Horst, F. B. Dyer, and M. Tuley, “Radar sea clutter model,” in *Proc. of the Intl. IEEE AP/S URSI Symposium*, pp. 6–10, 1978.

About FFI

The Norwegian Defence Research Establishment (FFI) was founded 11th of April 1946. It is organised as an administrative agency subordinate to the Ministry of Defence.

FFI's mission

FFI is the prime institution responsible for defence related research in Norway. Its principal mission is to carry out research and development to meet the requirements of the Armed Forces. FFI has the role of chief adviser to the political and military leadership. In particular, the institute shall focus on aspects of the development in science and technology that can influence our security policy or defence planning.

FFI's vision

FFI turns knowledge and ideas into an efficient defence.

FFI's characteristics

Creative, daring, broad-minded and responsible.

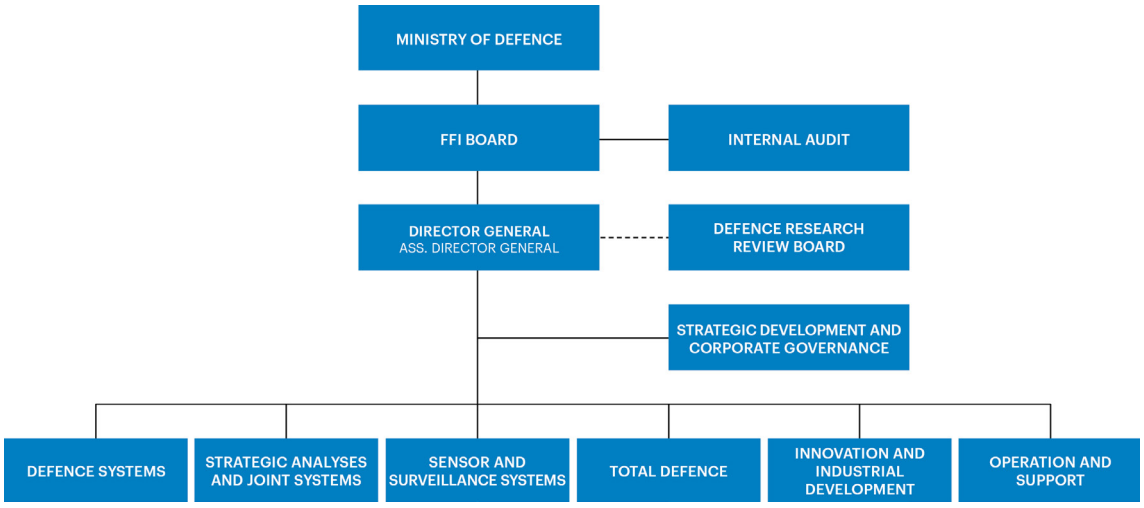

Forsvarets forskningsinstitutt (FFI)
Postboks 25
2027 Kjeller

Besøksadresse:
Kjeller: Instituttveien 20, Kjeller
Horten: Nedre vei 16, Karljohansvern, Horten

Telefon: 91 50 30 03
E-post: post@ffi.no
ffi.no

Norwegian Defence Research Establishment (FFI)
PO box 25
NO-2027 Kjeller
NORWAY

Visitor address:
Kjeller: Instituttveien 20, Kjeller
Horten: Nedre vei 16, Karljohansvern, Horten

Telephone: +47 91 50 30 03
E-mail: post@ffi.no
ffi.no/en